

Raman sideband cooling of single Na atoms to 3D vibrational ground state

.....
Harvard Department of Physics
(Dated: May 22, 2017)

We report Raman sideband cooling of a single neutral Sodium atom to its three-dimensional vibrational ground state in an optical tweezer. Despite having a very large Lamb-Dicke parameter, high initial temperature and large differential AC Stark shift in the excited state, after applying a cooling sequence for a hundred milliseconds, we observed a ground state preparation fidelity of 70% using sideband thermometry. We demonstrated that Raman sideband cooling to vibrational ground state is applicable to systems where tight confinement or low initial cooling is hard to achieve. For example, the result provides new opportunities to achieve much lower temperatures in cold molecules with direct laser cooling.

Why do we need to cool (for STIRAP/transfer to molecular state)

* Pure initial state

* Small wavefunction span

We achieve the high ground state preparation fidelity needed for molecule formation using Raman sideband cooling. The process consists of multiple cycles of laser pulses to manipulate the internal and vibrational states of the atoms. Figure 1A shows the schematic of the energy levels and the cooling sequence in our setup. Each cooling cycle starts with the Sodium atom in the $|F = 2, m_F = -2\rangle$ ground electronic state and a certain vibration state n . In the first step, a Raman pulse drives a transition to the vibrational state $n - \Delta n$ to reduce the vibrational energy while also changing the internal state to $|F = 1, m_F = -1\rangle$. In the second step, which finishes the cooling cycle, an optical pumping pulse bring the atom back to the $|F = 2, m_F = -2\rangle$ state to take away the entropy. The second step could also change the vibrational state of the atoms which could cause heating. The possibility for this to happen for an atom in the vibrational level n is approximately proportional to the effective Lamb-Dicke parameter $\eta_{eff}^{OP} = \sqrt{2n + 1}\eta^{OP}$ where $\eta^{OP} = ???$ is the Lamb-Dicke parameter for optical pumping. The geometry of the relevant beams (???and their polarizations) is showed in figure 1B. The optical tweezer has one weakly confined axial direction (axis 1) and two more strongly confined radial directions (axis 2 and 3). Multiple pairs of beams are used to drive the Raman transition during cooling in order to isolate and maximize the coupling to different trap axis.

Although Raman sideband cooling to vibrational ground state has already been successfully implemented on neutral atoms in other experiments using heavier species like Rubidium [????] and Cesium [????], such experiments generally use good polarization gradient cooling and a tight confinement to achieve a small Lamb-Dicke parameter and effective Lamb-Dicke parameter. However, this regime is harder to achieve with Sodium atoms, creating additional challenges for us to realize

ground state cooling. On the other hand, since these conditions can also be difficult to meet for other interesting systemd like directly laser cooled molecules, the techniques we use to overcome these challenges could be useful for a wider variety of systems.

As mentioned previously, in order to perform Raman sideband cooling efficiently and minimize the heating during the optical pumping, we need to have a low initial temperature and a small Lamb-Dicke parameter. However, since the Lamb-Dicke parameter η is inversely proportional to \sqrt{m} (???) where m is the mass of the atom, it is larger for Sodium given the same trap depth (???). With 45mW of power at the focus of the trap, we measured a trapping frequency of $\{\omega_1, \omega_2, \omega_3\}/2\pi = \{67, 420, 580\}$ kHz which corresponds to optical pumping Lamb-Dicke parameters of $\{\eta_1^{OP}, \eta_2^{OP}, \eta_3^{OP}\} = \{???, ???, ???\}$. Moreover, due to the unresolved(?) hyperfine structure in the $3^2P_{3/2}$ manifold, the sub-doppler cooling in Sodium is also less efficient and we start the Raman sideband cooling with a initial temperature of $40\mu K$. Combined with the high Lamb-Dicke parameters, this gives us a initial effective optical pumping Lamb-Dicke parameters of $\{\eta_{1eff}^{OP}, \eta_{2eff}^{OP}, \eta_{3eff}^{OP}\} = \{???, ???, ???\}$ As a result, there is a very high probability of heating during the optical pumping step (figure 2B) causing a 30% average heating probability during optical pumping in the weakly confined axial direction. Fortunately, the high Lamb-Dicke parameters also provide us tools to overcome this issue. From our geometry, the Lamb-Dicke parameters for Raman transitions are $\{\eta_1^R, \eta_2^R, \eta_3^R\} = \{???, ???, ???\}$. As shown in figure 2A, the high Raman Lamb-Dicke parameters causes a strong coupling to higher orders of cooling sidebands, especially for high vibrational states. This enables us to cool atoms in high vibrational states by driving on high order Raman sidebands, removing more vibrational energy in a single cooling pulse and offsetting the effect of strong heating. Since the heating probability is higher for high vibrational states, cooling on these high order sidebands can greatly suppress the high heating during optical pumping during the initial cooling. Since the coupling strength of different orders do not reach their

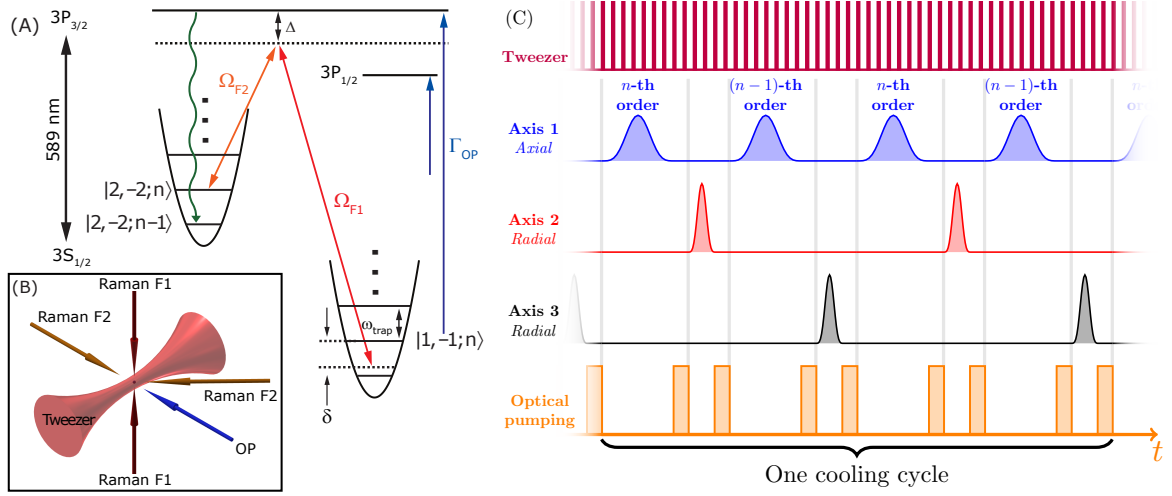


FIG. 1. (A) Energy diagram. D1 OP (B) Beam directions and polarizations (C) Sequence description

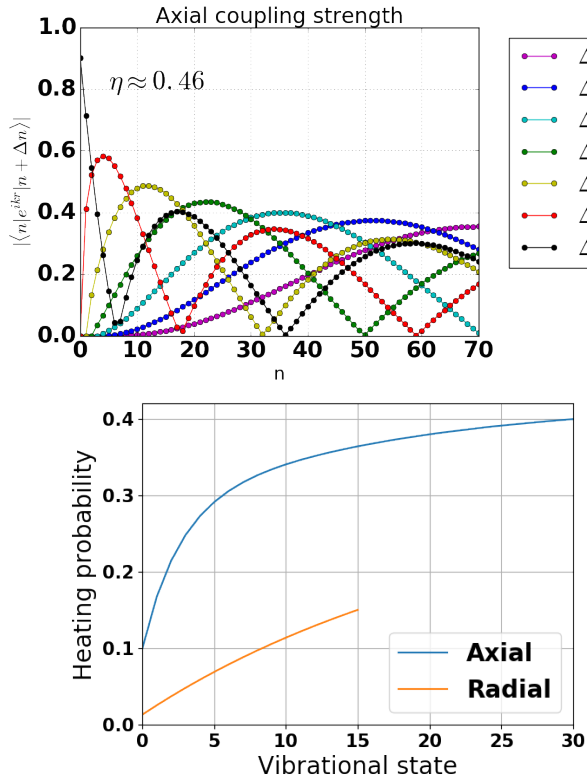


FIG. 2. (A) Matrix elements as a function of n and Δn (showing complex dependency and zeros) (B) State changing probability. Large and increases as n gets larger

minimums at the same time, using multiple orders of vibrational sidebands for cooling also avoids accumulation of population near the coupling minimum of a particular order, which improves the overall efficiency of the cooling process.

In addition to improving the cooling efficiency, the

large Raman Lamb-Dicke parameters η^R also creates difficulties for measuring the temperature. Traditional sideband thermometry uses the ratio of the cooling and heating sidebands to measure $\bar{n}/(\bar{n} + 1)$, which relies on the coupling strength to be proportional to \sqrt{n} . However, since we are not in the Lamb-Dicke regime, the coupling strength deviates from this simple scaling rule quickly as already shown in figure 2A, causing the normal sideband thermometry to break down. In order to solve this problem, when the atom temperature is still high, we measure the heights of multiple sidebands to make sure no population is hidden at the minimum of one sideband order. And when the atom is cooled down, we estimate the temperature and ground state population under the assumption that only a few states are populated. This result is then verified using independent measure of Rabi flopping on the carrier and heating sidebands since they provide more information about the distribution of coupling strength.

Another issue caused by the high initial temperature is trap anharmonicity. Although the potential near the center of a focused Gaussian beam can be approximated by a harmonic trap, when a large number of levels are populated due to high initial temperature the anharmonicity of the trap can lead to broadening of the sideband and the decrease of the sideband signal. In our setup, this effect limits the Rabi frequency of the Raman pulse on the radial sidebands to be no lower than tens of kilo-Hertz in order to drive atoms in different vibrational states equally.

Finally, another important

Taking all the features of our system into account, we use a Monte-Carlo simulation to verify the validity of our method and explore the large parameter space for the cooling sequence. In the simulation, we can observe the high heating rate due to the high Lamb-Dicke parameters and confirm that high order of Raman sideband can be used to suppress this effect and reduces the vibrational

energy of the atom faster. We also use the simulation to find a robust cooling strategy. As shown in figure (?), we found that instead of cooling on only one sideband order at a time, it is generally more efficient to alternate the cooling pulse between two neighboring orders. A cooling sequence like this minimizes the accumulation of atom in a state not addressed by a particular sideband order.

For the more tightly confined radial directions, we starts the cooling with $\{\bar{n}_2, \bar{n}_3\} = \text{????, ????}$. The sideband spectra of the initial distribution is shown in figure 3A where we can clearly see the first order heating, first order cooling and second order cooling sidebands. After applying about 1000 cooling pulses cooling in all three dimentions starting with cooling on the radial second order, the Raman spectrum with the same parameter is shown in figure 3B, where both cooling orders are suppressed. We can estimate the ground state probability in each direction based on the height of the first order cooling and heating sideband and the absence of the second order cooling sideband to be Due to the complexity of the sideband structure, we also use the Rabi flopping on the carrier and heating sideband as a independent measurement of the ground state population and gets, showing good agreement between the two methods. (????? figure 3C and 3D)

As mentioned previously, the axial direction is much less confined and therefore has a much higher effective Lamb-Dicke parameter of $\sqrt{n}\eta_{Raman1} \approx 2.4$. The Raman spectrum before applying Raman sideban cooling is shown in figure 4A where we can see clearly resolved Raman cooling sidebands up to the 8th order suggesting that we have many vibrational states populated in this direction.

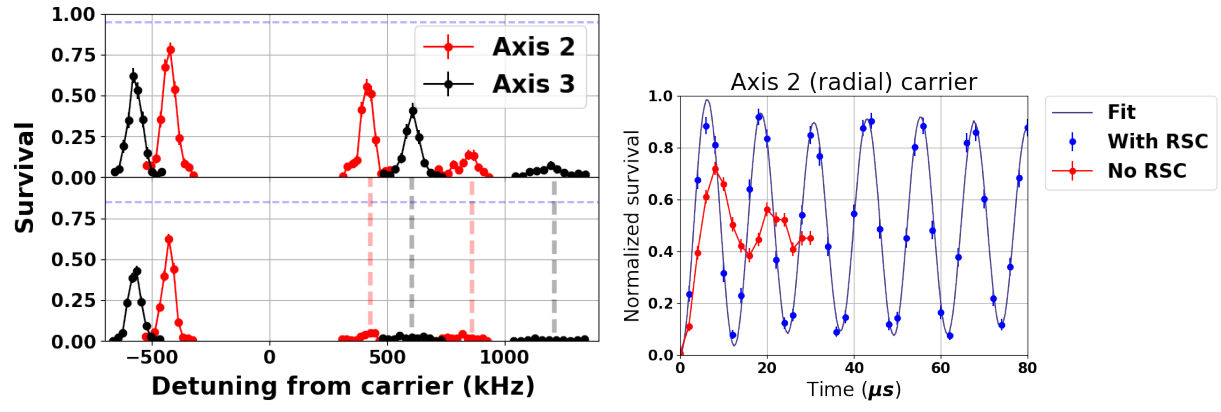


FIG. 3. (A) (B)

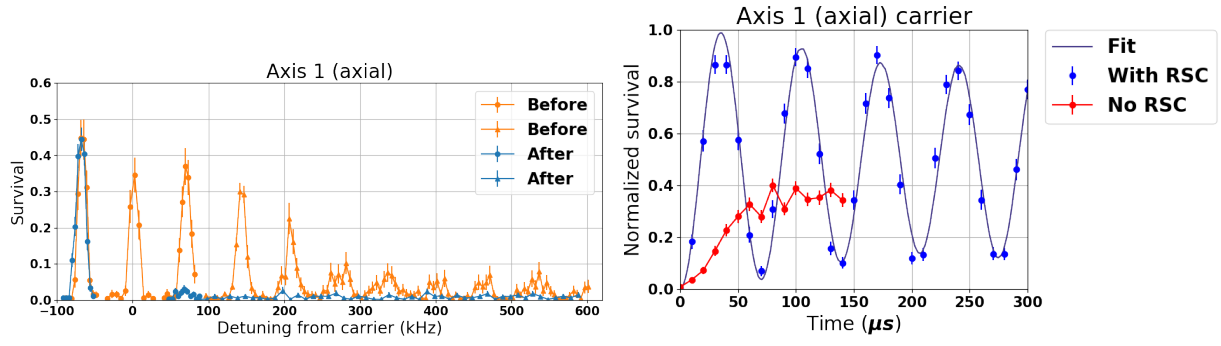


FIG. 4. (A) (B)